LINC00152 promotes Ovarian tumor progression and Predicts Poor Prognosis by inhibiting the ubiquitination of BCL6

Shunni Wang
Obstetrics and Gynecology Hospital of Fudan University https://orcid.org/0000-0001-5154-492X
Weiwei Weng
Fudan University Shanghai Cancer Center
Tingting Chen
Obstetrics and Gynecology Hospital of Fudan University
Midie Xu
Fudan University Shanghai Cancer Center
Ping Wei
Fudan University Shanghai Cancer Center
Jing Li
Obstetrics and Gynecology Hospital of Fudan University
Linghui Lu
Obstetrics and Gynecology Hospital of Fudan University
Yiqin Wang (yiqinwang11@icloud.com)

Research

Keywords: LINC00152, BCL6, ubiquitination, ovarian cancer

Posted Date: March 19th, 2020

DOI: https://doi.org/10.21203/rs.3.rs-17686/v1

Abstract

Background : Long non-coding RNA 00152 (LINC00152) has been found oncogenic in multiple somatic malignancies. But its roles in the ovarian cancer remain elusive. We aim to investigate its functions and mechanism in the ovarian tumor progression.

Methods: We used RNAscope and RT-qPCR assays to detect the LINC00152 levels in 152 pairs of ovarian tumor and paratumorous tissues, conducted in vitro and in vivo experiments to evaluate its biological functions, and performed RNA immunoprecipitation, RNA-pulldown, MS/LS analysis, mutant construction and ubiquitination assays to explore the LINC00152-BCL6 binding and regulation.

Results: LINC00152 was abnormally increased in the ovarian tumor tissues and its high expression predicted poorer survivals of patients; overexpression of LINC00152 promoted ovarian tumor proliferation and metastasis both in vitro and in vivo ; LINC00152 bond to Serine333 and Serine343 of BCL6 and then suppressed its ubiquitination; Finally, LINC00152 facilitated its oncogenic functions in a BCL6-mediated manner in ovarian cancer.

Conclusions: LINC00152 is the independent prognostic predictor of ovarian cancer; and the abnormal expression of LINC00152 facilitates ovarian tumor proliferation and invasion by suppress the ubiquitination of BCL6. Our data might be helpful in exploring the molecular mechanisms of lncRNA-protein interactions, and might provide the potential target for the tumor pharmacology of ovarian cancer.

Introduction

Ovarian cancer is responsible for approximately 5% of total cancer death with the proportion of less than 3% of all malignancies in females [1]. Despite the declined incidence and mortality in the past 3 decades, inconspicuous symptoms and signs still lead to delayed diagnoses at advanced stages with pelvic dissemination, causing the relatively low 5-year survivals as 42% for stage III and 26% for stage IV in the United States[2], revealing a highly aggressive nature that needs elaboration of underlying molecular process.

The long non-coding RNAs (lncRNAs, non-coding RNAs with sizes larger than 200bps) are associated with somatic tumor tumorigenesis and metastasis[3]. The non-coding RNA 00152 (LINC00152) is a lncRNA located at 2p11.2[4] and has been involved in cell proliferation[5], cell-cycle arrest[4],epithelial-mesenchymal transition[6] and cell invasion[7] to facilitate tumor initiation and progression. Our former study revealed that LINC00152 promoted tumor invasion and predicts poor prognosis in renal clear cell[8] and lung carcinomas[9]. Other studies have got similar findings in gastric cancer[10] and hepatic carcinoma[11], suggesting that LINC00152 might serve as a powerful oncogenic lncRNA in somatic malignancies. Researchers have found that LINC00152 forms the loop feedback with FOXM1 to stimulate tumor growth[12] and might serve as the ceRNA (competing endogenous RNA) to regulate miRNAs to fulfil its biological functions[5, 13, 14]. Although the impact of LINC00152 on ovarian cancer

proliferation has been implicated recently[15], its role and the exact molecular mechanism to regulate the ovarian tumor behavior need further investigation.

Ubiquitination is a posttranslational epigenetic mechanism that requires the conjugation of ubiquitin (Ub) to the lysine residues of specific substrate proteins via the enzyme-mediated transfer[16]. Now is known that ubiquitination is a crucial part of the molecular dysregulation in ovarian cancer[17]. And lncRNAs might facilitate tumorigenesis by regulating the process of the ubiquitination. It has been reported that lncRNA uc.134 represses CUL4A-mediated ubiquitination of LATS1 to inhibit the progression of hepatic cancer[18]. LncRNA-ANCR also has been reported to suppress the invasiveness of breast cancer cells by prompting the degradation of EZH2[19]. But it is unknown whether LINC00152 could affects ovarian tumorigenesis via the ubiquitin-related mechanism.

In the process of searching the correlation between LINC00152 and the ubiquitination-proteosome system, we found that B-cell CLL/lymphoma 6 (BCL6) might be the potential target of LINC00152. BCL6 is a highly conserved zinc finger transcriptional factor[20]and its degradation is mediated via the ubiquitination-proteosome system[21, 22]. We formerly have proved that BCL6 exerts oncogenic activities in ovarian cancer[23]. Based on these above, it is very likely that LINC00152- BCL6 regulation contributes to the ovarian tumor progression.

In this study, we aimed to investigate the role of LINC00152 in ovarian cancer via its possible regulation upon alterations of BCL6 degradation through the ubiquitin-proteosome system, and the potential influences of the LINC00152-BCL6 interaction on the biological behaviors and clinical outcomes.

Methods & Materials

Patient samples

152 pairs of tumor and paratumorous frozen tissues and paraffinized blocks with ovarian cancer were applied for this study from the biobank of Gynecological and Obstetrical Hospital of Fudan University from January 1st, 2012 to December 31st, 2016. None of the patients had received preoperative chemotherapy. The collected clinicopathological features included age, tumor size, staging, opposite ovary and fallopian tube involvement, lymph node and remote metastasis, and recurrence. All patients were staged based on the International Federation of Gynecology and Obstetrics (FIGO) staging system 2014. The follow-up interval was from the date of surgery to the date of death or the last clinical investigation. This study was approved by The Clinical Research Ethics Committee of Gynecology and Obstetrics Hospital of Fudan University. Written informed consent was obtained from all participants.

RNAScope detection of LINC00152 mRNA and Immunofluorescence

Detection of LINC00152 mRNA was performed using the RNAscope 2.5 HD Detection Reagent-BROWN (#322310, Advanced Cell Diagnostics, USA) and Multiplex Fluorescent (#323100) according to the

manufacturer's instructions. The DapB probe (#310043) was used as the negative control and Hs-PPIB (#313901) as positive control. Probe-LINC00152 (#18081B) was used for the test samples.

Transfected A2780, SKOV3, and negative control cells were fixed with 4% paraformaldehyde for 1h, penetrated with 0.5% Triton-100X (Sigma), and incubated with polyclonal rabbit anti-BCL6(Cellsignaling #14895) (1:100) and Probe-LINC00152 using the RNAscope RNA-protein confocal staining system. Then the cells were stained with Alexa Fluor 546 (red) along with Alexa Fluor 488 (green) (ACD, U.S.A.) as well as DAPI (Invitrogen, U.S.A.) for DNA staining.

Images were taken at 40x and 80x magnification using the BX45 (Olympus, Japan) light microscope, Leica inverted fluorescence microscope with ProgRes Image Capture Software (JENOPTIK Optical System, Jena, German) & Leica Confocal LAS-AF SP5 System. Dark-brown, punctuate dots in the nucleus and/or cytoplasm under the light microscope, and green (Fluor 488) signals under the fluorescence systems were considered positive for LINC00152. Red (Fluor 546) signals were considered positive for BCL6. The slides were evaluated by two pathologists blinded to the morphological diagnoses in order to exclude any possible influences of the morphology.

In vivo xenograft and metastasis models

Female BALB/c-nu mice (4-5 weeks of age, 18-20g) were maintained under specific pathogen-free conditions in the Experimental Animal Department of Fudan University. All of the experimental procedures involving animals were undertaken in accordance with the institute guidelines. 1×10^7 Lenti-NC, Lenti-LINC00152, Lenti-shC, Lenti–shLINC00152, Lenti-LINC00152-NC(BCL6), Lenti-BCL6-NC(LINC00152 Lenti-LINC00152-BCL6 and Lenti-LINC00152-BCL6$^{S333A/S343A}$ stably infected SKOV3 cells were injected s.c. into the flank regions of 8-week old BALB/c female nude mice (n=4 per group) and allowed to grow for 24-30 days. All the mice were euthanized and the xenografts were excised out and measured. The tumor volumes were calculated using the formula $½\times r1^2\times r2$ (r1<r2).

For the intraperitoneal tumor metastasis models, 8×10^6 SKOV3 cells stably infected with Lenti-NC or Lenti-LINC00152 were injected intraperitoneally (i.p.) (n= 3 per group). The abdominal circumferences of the mice were measured every 2 days. All the mice were anesthetized and sacrificed. The xenografts were excised and measured. The tumor volumes were calculated using the formula $½\times r1\times r2$ ($r1<r2$). The intraperitoneal organs (livers, peritoneal membranes, and intestines, etc.) were excised and examined for the implanted lesions followed by sampling. All the tissues were fixed and embedded with paraffin. Hematoxylin& Eosin staining was used to observe the lesions through a microscope.

Biotin pull-down assays and mass spectrometry

The LINC00152 and its antisense plasmid were linearly cut, transcribed, and biotin-labeled *in vitro* with Bio-16-UTP (Life Technologies) using a MAXIscript T7 Transcription Kit (Life Technologies). Protein–RNA interactions were carried out using a Pierce Magnetic RNA-Protein Pull-Down Kit (Life Technologies) with the lysates of H293T and CAOV3 cells. The FLAG-BCL6 protein complexes were fractionated by SDS-

PAGE, followed by Prussian blue staining. The Prussian blue-stained gel bands were treated with sequencing-grade trypsin (Lot. V5280, Promega, USA). The resulting peptides were analyzed by nano-HPLC-MS/MS with online desalting with a FAMOS autosampler. Electrospray ion trap MS was performed using an LTQ linear ion trap mass spectrometer (Thermo Finnigan). The fragment spectra were analyzed using the National Center for Biotechnology Information nonredundant protein database using Mascot (Matrix Science) and Sequest (Thermo Scientific). The base peak and the candidate proteins pulled down by LINC00152 were listed in the Supplementary Information.

Statistical analysis

Each experiment was performed in triplicate, and survival data were shown as the median following time, and other data were presented as the mean ±SD. All statistical analyses were performed using SPSS 20.0 (IBM, SPSS, Chicago, IL, USA). Student's t-test and one-way ANOVA were used in either 2 or multiple groups for statistical significance. Poison correlation and Spearman rank order were used to analyze the correlations; disease-free survival (DFS) and disease-specific survival (DSS) curves were calculated with the Kaplan-Meier method and were analyzed with the log-rank test. The DFS rate was calculated from the date of surgery to the date of progression (local and/or distal tumor recurrence) or the date of death. The DSS rate was defined as the length of time between the diagnosis and death or last follow-up. Univariate analysis and multivariate models were fit using a Cox proportional hazards regression model. All tests were 2-sided, and $P<0.05$ was considered statistically significant.

Other methods used in this study are listed the Supplementary Information.

Results

LINC00152 is upregulated in ovarian cancer and predicts poor clinical outcomes

We first detected the levels of LINC00152 mRNA using RNAscope and RT-qPCR in 152 pairs of ovarian cancer and adjacent normal tissues (ANTs). The RNAscope showed that LINC00152 was positively stained in the tumor lesions while negative in the ANTs (**Figure 1A**). 64.65% of high-grade serous, 72.00% of endometrioid, 23.81% of clear cell type and 28.57% of mucinous subtype showed positive expression of LINC00152 (**Figure 1A, Table 1**). The RT-qPCR results showed that the mRNA level of LINC00152 was significantly higher in the 152 malignant lesions than in the paired paratumorous areas ($P<0.001$, **Figure 1B**), corresponding to the result of 2 independent cohorts from TCGA (www.cbioportal.com, n=440, **Supplementary Figure S1A-B**).

Next we analyzed the correlation between LINC00152 expression and the clinicopathologic parameters of patients with ovarian cancer both in our cohort and the cohorts from TCGA. The LINC00152 levels were positively correlated with the advance of FIGO stage ($P<0.001$, **Figure 1C**), consistent with the results of cohorts from TCGA (n=440, **Supplementary Figure S1C**). Moreover, the LINC00152 mRNA levels were increased in the patients with larger tumor sizes (>5cm in diameter, $P=0.009$, **Table 1**), vascular invasion ($P=0.015$, **Table 1**) and lymph node metastasis ($P<0.001$, **Table 1**). Notably, the expression of LINC00152

detected by RT-qPCR was not correlated with the histological subtypes of ovarian cancer (high-grade serous, endometrioid, clear cell and mucinous types) (**Table 1**). Within the endometrioid subtypes, the LINC00152 mRNA levels were not correlated with the tumor grades (**Table 1**). When LINC00152 was divided into the high and low expression groups by the median value according to the previous studies[22,23], the distributions of patients with advanced FIGO stage (P<0.001, **Figure 1C**), larger tumor size (P=0.004, **Supplementary Figure S1D**) and with lymph node metastasis (P<0.001, **Supplementary Figure S1E**) were correlated with LINC00152 high expression.

We then elucidated the impacts of LINC00152 on patients' clinical outcomes. The total median follow-up time for the patients who were still alive at the endpoint for analysis was 31.50 months. The median follow-up time for the patients who were still alive at the endpoint was 29.50 months in the high LINC00152 expression group and 32.00 months in the low expression group. The LINC00152 levels were significantly increased in the patients with recurrence (P=0.010, **Table 1**). When dividing LINC00152 into the high and low expression groups by the median value, high LINC00152 expression was associated with recurrence (P<0.001, **Figure 1D**). The Kaplan-Meier analysis showed that patients with high LINC00152 expression (n=76) had significantly shorter DFS (P=0.004; **Figure 1E**) and DSS rates (P=0.005; **Figure 1F**) compared with those with low expression (n=76). These results corresponded to that of the cohorts from TCGA which illustrated that high LINC00152 expression was also correlated with poorer overall survivals (OS, P=0.035, n=440, **Supplementary Figure S1F**). Then we performed the univariate Cox analysis and found that lymph node metastasis, FIGO stage and LINC00152 expression were all correlated with the DFS (P=0.004, **Supplementary Table S1**) and DSS (P=0.002, **Supplementary Table S2**). But after the multivariate analysis using the Cox proportional hazards model, the LINC00152 level remained to be an independent predictor for DFS (P=0.029, **Supplementary Table S1**) and DSS (P=0.040, **Supplementary Table S2**) along with FIGO stage (P=0.026 for DFS，**Supplementary Table S1**; P=0.048 for DSS, **Supplementary Table S2**). Furthermore, we compared the prognostic value of LINC00152 for DFS and DSS with the other independent risk factor FIGO stage using receiver operating characteristics (ROC) curves. It turned out that both LINC00152 expression and FIGO stage showed similar AUC (area under curve) for DFS (P<0.01, **Figure 1F**) and DSS (P<0.01, **Figure 1F**), but the combination of these two independent predictors presented superior prognostic value (P<0.01, **Figure 1F**). All these together suggest that abnormal LINC00152 expression predicts poor clinical outcomes of patients with ovarian cancer, and combined LINC00152 with FIGO stage could serve as a more sensitive and specific prognostic marker for ovarian cancer.

LINC00152 promotes ovarian cancer cell proliferation and metastasis *in vitro* and *in vivo*

To further study the biological effects of LINC00152 on ovarian cancer, we next detected LINC00152 mRNA levels in a panel of cell lines and chose the candidate A2780 and SKOV3 cells for overexpression while ES-2 and CAOV3 cells for knockdown (**Supplementary Figure S2A**). The efficiencies of overexpression and interference were confirmed by RT-qPCR (P<0.01, **Supplementary Figure S2B**). Then we investigated the potential effect of LINC00152 on ovarian cancer *in vitro* and *in vivo*. The CCK8 counting and colony-forming assays showed that overexpression of LINC00152 stimulated proliferations

of A2780 and SKOV3 cells (P<0.05, **Figure 2A-B**), while knockdown of LINC00152 decelerated the growth of CAOV3 and ES-2 cells *in vitro* (P<0.05, **Figure 2A-B**). Similarly, the transwell and wound-healing assays showed that overexpression of LINC00152 enhanced the mobilization and penetration of SKOV3 and A2780 cells while knockdown of LINC00152 reduced the invasion and migration of CAOV3 and ES-2 cells (P<0.05, **Figure 2C-D**). Finally, the *in vivo* xenograft models showed that overexpression of LINC00152 accelerated the growth and enlarged the sizes of xenografts (P<0.05, **Figure 2E**), and the metastasis models showed that overexpression of LINC00152 added the abdominal circumferences of nude mice and caused more metastatic lesions in the abdominal organs (**Figure 2F**). All these results suggest that LINC00152 promotes ovarian tumor growth and invasion both *in vitro* and *in vivo*.

LINC00152 interacts with the co-localized BCL6 protein and elevates its level

Since we previously reported that lncRNAs interact with proteins to fulfill their biological functions, we first used LC-MS/MS spectrometric analyses to analyze the purified LINC00152 containing complex pulled down by 3 independent biotin RNA-protein pulldown assays in CAOV3 cells. The mass spectrometry identified that the complex contained the peptides of BCL6 (**Figure 3A, Supplementary Figure S3A and Table S3**), which was also confirmed by the western blotting result of RNA-protein pulldown products (**Figure 3A**). Besides, we performed the RNA immunoprecipitation assay using CAOV3 cells and H293T cells, and again LINC00152 was found to be bound by the endogenous BCL6 (**Figure 3B**), suggesting that LINC00152 can bind directly to BCL6 protein.

Then we analyzed the data of two cohorts in the TCGA and found that both LINC00152 and BCL6 genes were amplified (**Supplementary Figure S3B**), and the mutual exclusivity of these two genes was co-occurrence (P=0.011, **Supplementary Figure S3C**). Back to our study, overexpression of LINC00152 elevated the protein levels of BCL6 in A2780 and SKOV3 cells, while knockdown of LINC00152 reduced the protein levels of BCL6 in CAOV3 and ES-2 cells (**Figure 3C**). However, the interference of LINC00152 failed to affect the mRNA levels of BCL6 accordingly (**Figure 3D**), suggesting that the regulatory effect of LINC00152 on BCL6 is on the posttranslational level.

To further confirm the localization of LINC00152 and BCL6 protein, we performed RNA-Protein dual staining using the RNAscope technique (ACD, USA) in ovarian cancer tissues and tumor cell lines. It turned out that in the ovarian high-grade serous and endometrioid carcinoma tissues, the LINC00152 and BCL6 protein were expressed majorly in the nucleus (**Figure 3E**), but the more sensitive immunofluorescence showed that there was still a minority of LINC00152 and BCL6 proteins localized in the cytoplasm in spite of the majority found in the nucleus (**Figure 3F**). The following immunofluorescence and nuclear-cytoplasmic RT-qPCR/western blotting assays in both CAOV3 and ES-2 cells also proved that LINC00152 and BCL6 protein were co-expressed mainly in the nucleus but slightly in the cytoplasm (**Supplementary Figure S3D-S3E**). Overexpression of LINC00152 in A2780 and SKOV3 cells enhanced the expressions of BCL6 protein both in the nucleus and cytoplasm by the immunofluorescence and RT-qPCR/western blotting assays (**Figure 3G-3H**). All these together suggest that LINC00152 interacts with the co-localized BCL6 protein and elevates its level in ovarian cancer.

LINC00152 elevates the level of BCL6 protein by binding its specific sites and suppressing its ubiquitination

Because LINC00152 changed the expression of BCL6 on the protein level but not the mRNA level (**Figure 3C-D**), we assumed that LINC00152 might regulate BCL6 post-translationally. To confirmed this, we first used the protein inhibitor MG132 to successfully rescue the reduced levels of BCL6 protein caused by the knockdown of LINC00152 in CAOV3 and ES-2 cells (**Figure 4A**). In the meantime, we found that overexpression of LINC00152 prolonged the semi-life of BCL6 protein under the influence of the eukaryotic protein synthesis inhibitor Cycloheximide (CHX) in A2780 and SKOV3 cells (**Figure 4B and Supplementary Figure S4A**, $P<0.05$). Furthermore, the ubiquitination assay confirmed that overexpression of LINC00152 could increase the levels of endogenous poly-ubiquitinated BCL6 in CAOV3 (**Figure 4C**) and ES-2 cells (**Supplementary Figure S4B**) as well as the exogenous poly-ubiquitinated BCL6 in SKOV3 (**Figure 4D**) and A2780 cells (**Supplementary Figure S4C**). Taken together, these data suggest that LINC00152 elevates the protein level of BCL6 by inhibiting its ubiquitination.

Since the previous studies have provided several potential sites correlated with degradation of BCL6[24], we constructed the corresponding plasmids of mutated and truncated BCL6 (**Figure 4E**). It turned out that MG132 inhibited the degradation of wild-type BCL6 and the truncated BCL6 proteins including $BCL^{\Delta N(1-121aa)}$, $BCL^{\Delta N(300-450aa)}$ and $BCL^{\Delta N(520-680aa)}$ but not the mutant $BCL6^{S333A/S343A}$ (**Figure 4F**). In contrast, under the influence of CHX, the wild-type BCL6 and all the truncated proteins of BCL6 ($BCL^{\Delta N(1-121aa)}$, $BCL^{\Delta N(300-450aa)}$ and $BCL^{\Delta N(520-680aa)}$) were degraded but not the mutant $BCL6^{S333A/S343A}$ (**Figure 4G**). Furthermore, overexpression of LINC00152 only failed to elevate the protein level of mutant $BCL6^{S333A/S343A}$ (**Figure 4H**). Finally, the RNA binding protein immunoprecipitation(RIP) assay showed that the binding between LINC00152 and mutant $BCL6^{S333A/S343A}$ was significantly reduced compared with the wild-type BCL6 ($P<0.01$, **Figure 4I**). All these data suggest that LINC00152 binds to Ser333/Ser343 of BCL6 protein and elevates its protein level by suppressing its ubiquitination.

LINC00152 promotes ovarian cancer progression in a BCL6-mediated manner

To investigate whether LINC00152 exhibited its functions in ovarian cancer in a BCL6-mediated manner, we first observed the effect of simultaneous overexpression of LINC00152 and knockdown of BCL6. It was shown that knockdown of BCL6 in the LINC00152-overexpressing A2780 and SKOV3 cells led to the reduction of metastasis-related genes such as SNAIL and N-CADHERIN, as well as the proliferation-related gene CCNB1 (**Figure 5A**). The CCK-8, colony-forming and EdU assays showed that overexpression of LINC00152 stimulated the proliferation of SKOV3 and A2780 cells but impaired by simultaneous knockdown of BCL6 ($P<0.05$, **Figure 5B**). The transwell assay proved that knockdown of BCL6 partially attenuated the effects of overexpression of LINC00152 on ovarian cancer cell invasion ($P<0.05$, **Figure 5C**). Consistently, the *in vivo* xenograft models confirmed that knockdown of BCL6 partially abolished the accelerated tumor growth and the increased tumor size/weight induced by overexpression of LINC00152 ($P<0.05$, **Figure 5D**).

In addition, we identified the indispensability of the interaction of LINC00152 with BCL6 on the biological functions of ovarian cancer. The CCK8, colony-forming and EdU assays revealed that the enhanced proliferation and invasion of SKOV3 cells induced by overexpression of LINC00152 could be further boosted by co-overexpression by the wild-type BCL6 but not the mutant $BCL6^{Ser333/Ser343}$ (P<0.05, **Figure 6A-C**), and the xenograft models also indicated that the accelerated growth speed and increase size/weight of xenografts induced by overexpression of LINC00152 could be amplified by co-overexpression of the wild-type BCL6 but not the mutant $BCL6^{Ser333/Ser343}$ (P<0.05, **Figure 6D**). All these data suggest that LINC00152 prompts ovarian tumor progression in a BCL6-mediated manner, and their interaction is essential to the functional fulfilment of LINC00152.

Discussion

In this study, we found that the mRNA level of LINC00152 was abnormally increased in the ovarian tumor tissues and cell lines accompanied with dysregulated biological functions, poorer clinical outcomes and facilitated cell proliferation and metastasis. Moreover, we provided the first-hand evidence of LINC00152 regulation on the degradation of BCL6, which directly promoted the progression of ovarian cancer. Thus, our study reveals the target molecules of LINC00152 and the molecular mechanisms of BCL6-related lncRNAs in the tumorigenesis of ovarian cancer.

Located at 2p11.2, LINC00152 has been reported as an oncogenic lncRNA in multiple somatic malignancies[11, 27, 28]. We formerly found that LINC00152 predicted negative prognosis and prompted tumor invasion in the renal clear cell carcinoma and lung adenocarcinoma[8, 9]. In this study, we found the dysregulated increase of LINC00152 expression in ovarian cancer tissues as well as the relevance between its abnormal expression and poor prognosis. In addition, we found high LINC00152 expression was independently predicted the risks of poorer DFS and DSS, and the combination of LINC00152 and FIGO stage in ROC curve analysis could offer better predictive value of patients' survivals compared with FIGO staging or LINC00152 solely. Since the FIGO stage has been considered as the crucial risk factor for the prognosis of ovarian cancer[29], our data suggested that even in the patient at the same FIGO stage, introduction of LINC00152 expression for stratified analysis might offer more precise prediction of risks of recurrence and mortality, which might also partially offer clues to the difference of survivals in patients at same FIGO stages. Based on the occult invasiveness of ovarian cancer, it would be of clinical value to apply LINC00152 as the regular monitoring factor postoperatively for the patients. Future studies need to focus on the consistence of LINC00152 expression in serum with that in tissues that might ease the detection and monitoring methods.

The previous studies have found that LINC00152 could compete as a ceRNA with miRs to fulfil its functions in hepatic and cervical cancers[11, 15, 30, 31]. Besides, LINC00152 is related to the regulation of signaling pathways such as Wnt/β-Catenin pathway[12, 32]. In contrast, Our MS/LS data based on RNA-pulldown assays and in vitro experiments suggested that oncogenic BCL6 was the posttranslational

regulation target of LINC00152, and LINC00152 promoted ovarian tumor invasion and metastasis in a BCL6-mediated manner. We have reported that BCL6 facilitates ovarian tumor progression but its molecular regulation is unclear[23]. Although other studies have reported the possible links between BCL6 and lncRNAs[33], the details of underlying mechanisms still remains elusive. In this study, we found that LINC00152 directly bond to the degradation sites of BCL6 thus inhibiting its ubiquitination, accumulating the BCL6 protein level to exhibit tumorigenic activities. The degradation of BCL6 protein has been referred to the MAPK1-mediated phosphorylation of the Serine 333 and Serine 343 followed by the proteasome-mediated ubiquitination[26]. Alternatively, the BTB domain (N-terminal 32-99aa) might form dimers to induce the FBXL17-conducted degradation[34]. Based on these, we constructed truncated or point mutants of BCL6 in this study. It was interesting that LINC00152 had similar effects on the binding and accumulation of the wild-type BCL6 and the N-terminal truncated mutant, while LINC00152 nearly lost the ability of binding to the double-point mutant of BCL6 (S333A/S343A) and overexpression of LINC00152 failed to increase the protein level of $BCL6^{S333A/S343A}$. These results supported the possibility that LINC00152 might occupied the phosphorylated sites of BCL6 to inhibit its phosphorylation rather than interact with its BTB domain thus suppressed the degradation of BCL6. Although our results could not exclude the other possibilities of regulation patterns, we still offer clues to the nature and laws of lncRNA-protein interaction. In future we shall continue to focus on the LINC00152-BCL6 centered networks to widen the potential links to additional miRNAs and other lncRNAs.

Conclusion

In summary, our study suggests that LINC00152 is the applicable independent prognostic predictor of ovarian cancer, and its abnormal expression facilitates ovarian tumor proliferation and invasion by binding to the degradation-required sites of BCL6 to suppress its ubiquitination. Our data might be helpful with the exploration of molecular mechanisms of lncRNA-protein interactions, and might provide the potential target for the tumor pharmacology of ovarian cancer.

Abbreviations

LINC00152 long non-coding RNA 00152

lncRNAs the long non-coding RNAs

ceRNA competing endogenous RNA

BCL6 B-cell CLL/lymphoma 6

DFS disease-free survival

DSS disease-specific survival

ANTs adjacent normal tissues

Declarations

Ethics approval and consent to participate

The experiments were undertaken with the understanding and written consent of each subject and conformed to the standards set by the Declaration of Helsinki. The study were approved by ethics committee of Obstetrics and Gynecology Hospital of Fudan University.

Animal experiments were approved by the Shanghai Medical Experimental Animal Care Commission and carried out in accordance with fudan university laboratory animalsadministration.

Consent for publication

Not applicable.

Availability of data and materials

The datasets used and analysed during the current study are available from the corresponding author on reasonable request.

Disclosure of Potential Conflicts of Interest:

No potential conflicts of interest were disclosed.

Sponsorship

This study was supported by National Natural Science Foundation of China (No. 81602269).

Author contributions

WYQ was the sponsor and designed the project. CTT, XMD, WP, LJ and LLH were responsible for the part of experiments and analyzed the data. WSN and WWW organized the data, composed the paper and substantively revised it.All authors read and approved the final manuscript.

Acknowledgement

We thank staff of department of Pathology, Obstetrics and Gynecology Hospital of Fudan University for technical assistance.

References

1. Torre LA, Trabert B, DeSantis CE, Miller KD, Samimi G, Runowicz CD, et al. Ovarian cancer statistics, 2018. CA Cancer J Clin. 2018;68:284-96.
2. Siegel RL, Miller KD, Jemal A. Cancer statistics, 2019. CA Cancer J Clin. 2019;69:7-34.
3. Quinn JJ, Chang HY. Unique features of long non-coding RNA biogenesis and function. Nat Rev Genet. 2016;17:47-62.
4. Zhao J, Liu Y, Zhang W, Zhou Z, Wu J, Cui P, et al. Long non-coding RNA Linc00152 is involved in cell cycle arrest, apoptosis, epithelial to mesenchymal transition, cell migration and invasion in gastric cancer. Cell Cycle. 2015;14:3112-23.
5. Zhou Z, Huang F. Long Non-Coding RNA LINC00152 Regulates Cell Proliferation, Migration And Invasion In Esophageal Squamous Cell Carcinoma Via miR-107/Rab10 Axis. Onco Targets Ther. 2019;12:8553-67.
6. Cai Q, Wang Z, Wang S, Weng M, Zhou D, Li C, et al. Long non-coding RNA LINC00152 promotes gallbladder cancer metastasis and epithelial-mesenchymal transition by regulating HIF-1alpha via miR-138. Open Biol. 2017;7.
7. Reon BJ, Takao Real Karia B, Kiran M, Dutta A. LINC00152 Promotes Invasion through a 3'-Hairpin Structure and Associates with Prognosis in Glioblastoma. Mol Cancer Res. 2018;16:1470-82.
8. Wu Y, Tan C, Weng WW, Deng Y, Zhang QY, Yang XQ, et al. Long non-coding RNA Linc00152 is a positive prognostic factor for and demonstrates malignant biological behavior in clear cell renal cell carcinoma. Am J Cancer Res. 2016;6:285-99.
9. Zhang PP, Wang YQ, Weng WW, Nie W, Wu Y, Deng Y, et al. Linc00152 promotes Cancer Cell Proliferation and Invasion and Predicts Poor Prognosis in Lung adenocarcinoma. J Cancer. 2017;8:2042-50.
10. Yang T, Zeng H, Chen W, Zheng R, Zhang Y, Li Z, et al. Helicobacter pylori infection, H19 and LINC00152 expression in serum and risk of gastric cancer in a Chinese population. Cancer Epidemiol. 2016;44:147-53.
11. Ma P, Wang H, Sun J, Liu H, Zheng C, Zhou X, et al. LINC00152 promotes cell cycle progression in hepatocellular carcinoma via miR-193a/b-3p/CCND1 axis. Cell Cycle. 2018;17:974-84.
12. Wang W, Guo P, Chen M, Chen D, Cheng Y, He L. FOXM1/LINC00152 feedback loop regulates proliferation and apoptosis in rheumatoid arthritis fibroblast-like synoviocytes via Wnt/beta-catenin signaling pathway. Biosci Rep. 2019.
13. Liu P, He W, Lu Y, Wang Y. Long non-coding RNA LINC00152 promotes tumorigenesis via sponging miR-193b-3p in osteosarcoma. Oncol Lett. 2019;18:3630-6.
14. Wang H, Chen W, Yang P, Zhou J, Wang K, Tao Q. Knockdown of linc00152 inhibits the progression of gastric cancer by regulating microRNA-193b-3p/ETS1 axis. Cancer Biol Ther. 2019;20:461-73.
15. Chen P, Fang X, Xia B, Zhao Y, Li Q, Wu X. Long noncoding RNA LINC00152 promotes cell proliferation through competitively binding endogenous miR-125b with MCL-1 by regulating mitochondrial apoptosis pathways in ovarian cancer. Cancer Med. 2018;7:4530-41.

16. Popovic D, Vucic D, Dikic I. Ubiquitination in disease pathogenesis and treatment. Nat Med. 2014;20:1242-53.
17. Lu Y, Amleh A, Sun J, Jin X, McCullough SD, Baer R, et al. Ubiquitination and proteasome-mediated degradation of BRCA1 and BARD1 during steroidogenesis in human ovarian granulosa cells. Mol Endocrinol. 2007;21:651-63.
18. Ni W, Zhang Y, Zhan Z, Ye F, Liang Y, Huang J, et al. A novel lncRNA uc.134 represses hepatocellular carcinoma progression by inhibiting CUL4A-mediated ubiquitination of LATS1. J Hematol Oncol. 2017;10:91.
19. Li Z, Hou P, Fan D, Dong M, Ma M, Li H, et al. The degradation of EZH2 mediated by lncRNA ANCR attenuated the invasion and metastasis of breast cancer. Cell Death Differ. 2017;24:59-71.
20. Zhu L, Feng H, Jin S, Tan M, Gao S, Zhuang H, et al. High expressions of BCL6 and Lewis y antigen are correlated with high tumor burden and poor prognosis in epithelial ovarian cancer. Tumour Biol. 2017;39:1010428317711655.
21. Duan S, Cermak L, Pagan JK, Rossi M, Martinengo C, di Celle PF, et al. FBXO11 targets BCL6 for degradation and is inactivated in diffuse large B-cell lymphomas. Nature. 2012;481:90-3.
22. Hirata Y, Ogasawara N, Sasaki M, Mizushima T, Shimura T, Mizoshita T, et al. BCL6 degradation caused by the interaction with the C-terminus of pro-HB-EGF induces cyclin D2 expression in gastric cancers. Br J Cancer. 2009;100:1320-9.
23. Wang YQ, Xu MD, Weng WW, Wei P, Yang YS, Du X. BCL6 is a negative prognostic factor and exhibits pro-oncogenic activity in ovarian cancer. Am J Cancer Res. 2015;5:255-66.
24. Linardou H, Kalogeras KT, Kronenwett R, Kouvatseas G, Wirtz RM, Zagouri F, et al. The prognostic and predictive value of mRNA expression of vascular endothelial growth factor family members in breast cancer: a study in primary tumors of high-risk early breast cancer patients participating in a randomized Hellenic Cooperative Oncology Group trial. Breast Cancer Res. 2012;14:R145.
25. Qi P, Xu MD, Ni SJ, Shen XH, Wei P, Huang D, et al. Down-regulation of ncRAN, a long non-coding RNA, contributes to colorectal cancer cell migration and invasion and predicts poor overall survival for colorectal cancer patients. Mol Carcinog. 2015;54:742-50.
26. Niu H, Ye BH, Dalla-Favera R. Antigen receptor signaling induces MAP kinase-mediated phosphorylation and degradation of the BCL-6 transcription factor. Genes Dev. 1998;12:1953-61.
27. Liu D, Gao M, Wu K, Zhu D, Yang Y, Zhao S. LINC00152 facilitates tumorigenesis in esophageal squamous cell carcinoma via miR-153-3p/FYN axis. Biomed Pharmacother. 2019;112:108654.
28. Yu Y, Yang J, Li Q, Xu B, Lian Y, Miao L. LINC00152: A pivotal oncogenic long non-coding RNA in human cancers. Cell Prolif. 2017;50.
29. Ismail E, Kornovski Y. SURGICAL STAGING OF OVARIAN CANCER (I FIGO STAGE): IGCS-0018 Ovarian Cancer. Int J Gynecol Cancer. 2015;2:Suppl 1, 52.
30. Zheng L, Hu N, Zhou X. TCF3-activated LINC00152 exerts oncogenic role in osteosarcoma through regulating miR-1182/CDK14 axis. Pathol Res Pract. 2019;215:373-80.

31. Teng W, Qiu C, He Z, Wang G, Xue Y, Hui X. Linc00152 suppresses apoptosis and promotes migration by sponging miR-4767 in vascular endothelial cells. Oncotarget. 2017;8:85014-23.
32. Xian-Li T, Hong L, Hong Z, Yuan L, Jun-Yong D, Peng X, et al. Higher Expression of Linc00152 Promotes Bladder Cancer Proliferation and Metastasis by Activating the Wnt/beta-Catenin Signaling Pathway. Med Sci Monit. 2019;25:3221-30.
33. Shen J, Ma J, Li J, Wang X, Wang Y, Ma J. A long non-coding RNA LNBC3 facilitates non-small cell lung cancer progression by stabilizing BCL6. J Clin Lab Anal. 2019;e23122.
34. Mena EL, Kjolby RAS, Saxton RA, Werner A, Lew BG, Boyle JM, et al. Dimerization quality control ensures neuronal development and survival. Science. 2018;362.

Tables

Table 1 Relationship between LINC00152 expression and clinicopathologic parameters of ovarian cancer patients

Variables	Number (n = 152)	LINC00152 expression[a]	*P* value
Age (years)			0.125
<50	68	2.668 (0.186- 12.044)	
≥50	84	2.040 (0.181- 14.767)	
Tumor size			0.009*
< 5 cm	53	1.701 (0.186- 7.071)	
≥ 5 cm	99	2.652 (0.181-14.767)	
Histology			0.451
High grade Serous	99	2.511 (0.186-14.767)	
Endometrioid	25	2.148 (0.181-12.044)	
Clear cell	21	2.024 (0.226-7.002)	
Mucinous	7	1.133 (0.330-2.562)	
Grades (Endometrioid)			0.219
I	14	1.326(0.181-3.896)	
II	6	3.321(0.410-7.200)	
III	5	3.043(0.370-12.044)	
FIGO Stage[b]			0.001*
I	37	1.249 (0.181-3.937)	
II	13	1.303 (0.362-2.724)	
III	97	2.743 (0.186-14.767)	
IV	5	4.710 (1.340-7.445)	
Vascular invasion			0.015*
Absent	89	1.973 (0.186-11.114)	
Present	38	3.210 (0.226-12.044)	
The great Omentum invasion			0.068
Absent	57	2.040 (0.181-11.114)	
Present	61	2.813 (0.407-12.044)	
Lymphatic metastasis			<0.001*
Absent	55	1.597 (0.181-5.450)	
Present	37	4.736 (1.104-14.767)	
Recurrence			0.010*
Absent	107	1.911 (0.181-9.579)	
Present	45	3.295 (0.410-14.767)	

[a]Median of relative expression with minimum–maximum percentile is recorded in parentheses

[b]Tumor stage was obtained according to the FIGO (International Federation of Gynecology and Obstetrics) criteria.

* $P<0.05$

Figures

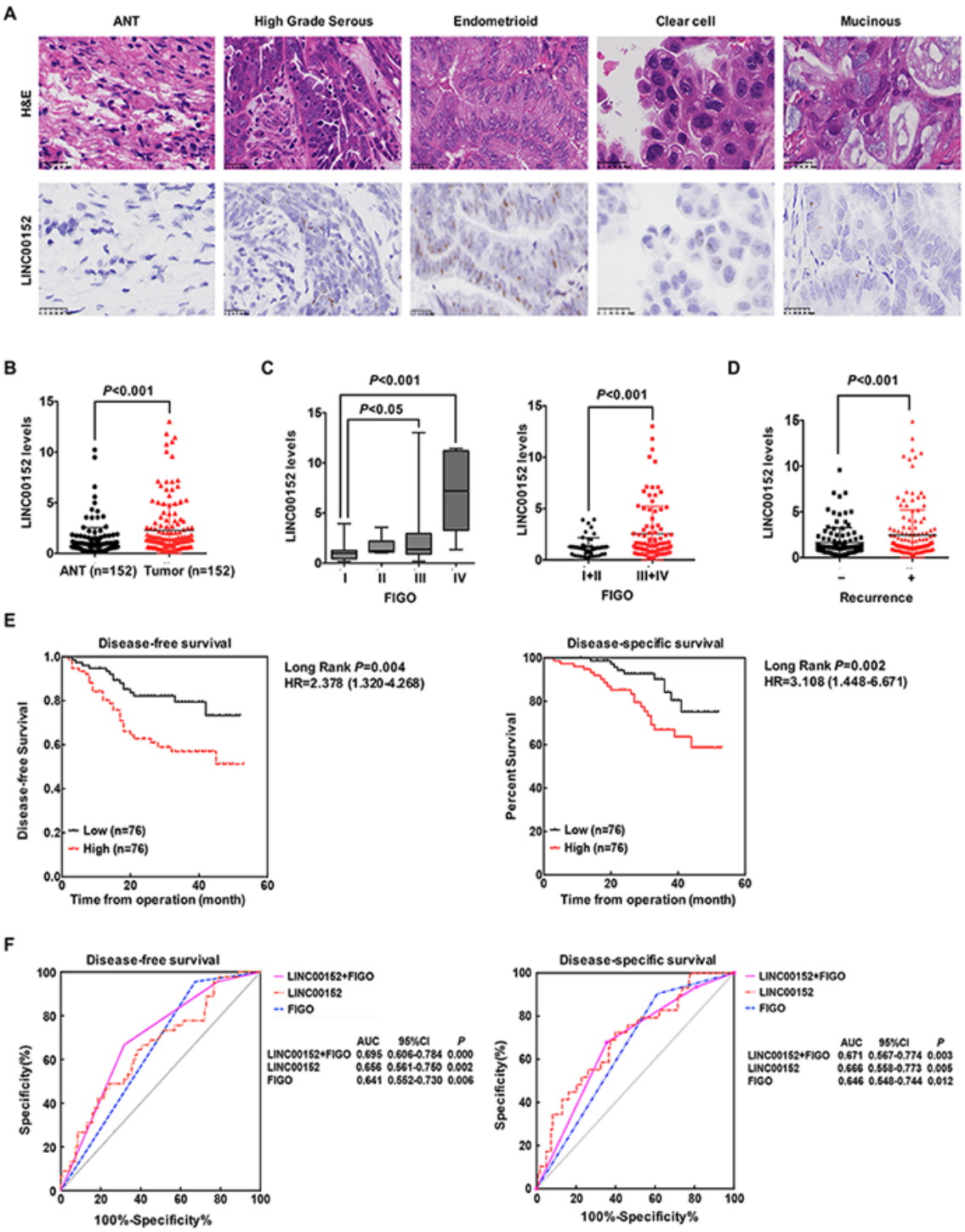

Figure 1

Figure 1

LINC00152 is upregulated in ovarian cancer and predicts poor clinical outcomes A. The expression of LINC00152 detected by in situ RNA hybridization in adjacent tumor tissues (ANTs) and different subtypes (high grade serous, endometrioid, clear cell and mucinous) of ovarian carcinomas. Scale bars=25 μm. B. The expression of LINC00152 detected by Real-time qPCR in 152 pairs of the adjacent tumor tissues (ANTs) and ovarian tumor tissues. $P<0.01$. C. The expression of LINC00152 detected by Real-time qPCR divided by FIGO stage in 152 cases of ovarian cancers. Left: The cases were divided into Stage I, II, III and IV. Right: The cases were divided into Stage I+II and Stage III+IV. $P<0.05$. D. The expression of LINC00152 detected by Real-time qPCR in cases with or without recurrences. $P<0.01$. E. The disease-free survivals (DFS) and the disease-specific survivals (DSS) of patients divided by expressions of LINC00152. The expression of LINC00152 was divided by the median value. The HR and the 95% CI were shown. $P<0.01$. F. The ROC curves for of LINC00152, FIGO and the combination of LINC00152 and FIGO for disease-free survivals (DFS) and the disease-specific survivals (DSS). The areas under curves (AUC) were shown. $P<0.01$.

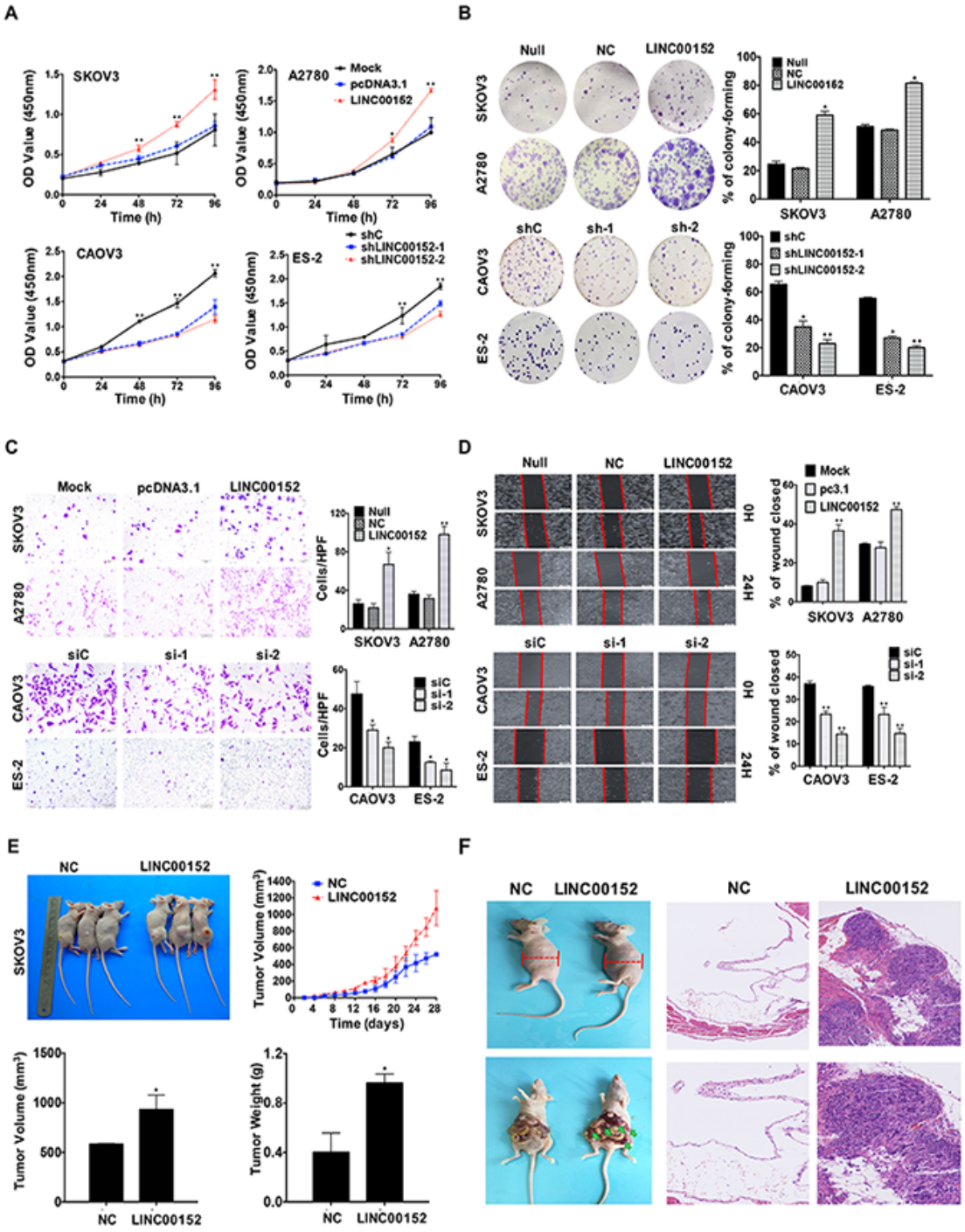

Figure 2

Figure 2

LINC00152 promotes ovarian cancer cell proliferation and metastasis in vitro and in vivo A. The CCK8 cell counting assays revealed the cell growth curves of NC and LINC00152-overexpressing SKOV3 and A2780 cells as well as shNC and LINC00152-knockdown ES-2 and CAOV3 cells at the indicated time points. Error bars are shown. *: P<0.01. **: P<0.05. B. Representative images of the colony-forming results of of NC and LINC00152-overexpressing SKOV3 and A2780 cells as well as shNC and LINC00152-knockdown ES-2

and CAOV3 cells for 14 days. *: P<0.01. **: P<0.05. C. Representative images (left) and quantification (right) of transwell invasion assays for the A2780 and SKOV3 cells overexpressed with LINC00152 as well as ES-2 and CAOV3 cells that were transfected with siLINC00152. Scale bars=200 μm. *: P<0.01. **: P<0.05. D. Representative images (left) and quantification (right) of wound-healing assays for A2780 and SKOV3 cells overexpressed with LINC00152 as well as ES-2 and CAOV3 cells that were transfected with siLINC00152. Scale bars=400 μm. *: P<0.05. **: P<0.01. E. Representative xenograft images (Top Left) and the statistical analytical graph (Top Right) of the xenograft tumor growth speed in nude mice injected with Lenti-NC and Lenti-LINC00152 overexpressing SKOV3 cells. The sizes (Bottom Left) and weights (Bottom Right) of xenografts were measured and analyzed. The error bars are shown. *: P<0.05. F. The representative abdominal circumferences of nude mice injected with Lenti-NC and Lenti-LINC00152 overexpressing SKOV3 cells (Top Left). The metastatic lesions were shown by arrows (Bottom Left). The H&E images of metastatic lesions were also shown (Right). Top Right: Scale bars=50 μm. Bottom Right: Scale bars=25 μm.

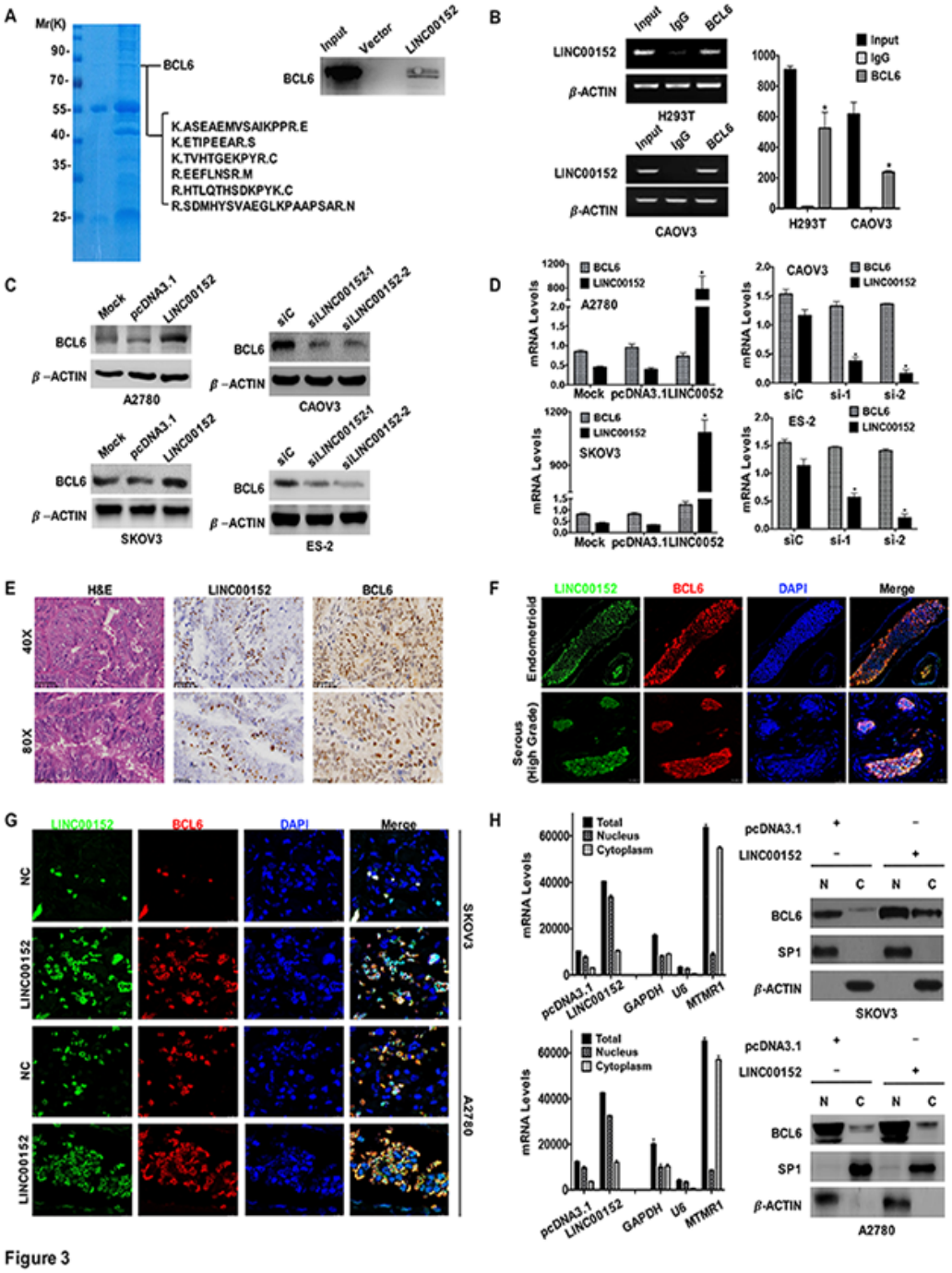

Figure 3

Figure 3

Figure 3. LINC00152 interacts with the co-localized BCL6 protein and elevates its level The Comassie blue stained SDS-PAGE presented the proteins pulled down by LINC00152 from CAOV3 cells, and the following LCMS/MS revealed the sequences from BCL6 in the pulldown complex (Left). The western blotting result by the independent RNA pulldown assays also showed that BCL6 was among the proteins binding to LINC00152 (Right). The RNA immunoprecipitation assays showed the interaction between LINC00152

and BCL6 protein in H293T and CAOV3 cells. The cell lysates were used as the inputs and IgG as the negative control. The RT-qPCR products were both analyzed with RNA electrophoresis (Left) and quantified by statistical graphs (Right). *: P<0.01. Western blot result showed the influences on BCL6 protein levels by either overexpression of LINC00152 in A2780 and SKOV3 cells or knockdown of LINC00152 in ES-2 and CAOV3 cells. The RT-qPCR results showed no influences on BCL6 RNA levels either by overexpression of LINC0052 in A2780 and SKOV3 cell, or knockdown of LINC00152 in ES-2 and CAOV3 cells. *: P<0.01. The RNAscope results stained by DAB showed the staining of LINC00152 and BCL6 protein in ovarian cancers. Top: Scale bars=50 μm. Bottom: Scale bars=25 μm. The dual staining of LINC00152 and BCL6 protein by RNAscope immunofluorescence in ovarian carcinomas of either emdometrioid (Top) or high-grade serous (Bottom) types. Scale bars=25 μm. The dual staining of LINC00152 and BCL6 protein by RNAscope immunofluorescence in NC and LINC00152-overexpressing A2780 and SKOV3 cells. Scale bars=10 μm. The nucleus-cytoplasm split RT-qPCR results of LINC00152 and western blot results of BCL6 in NC and LINC00152-overexpressing A2780 and SKOV3 cells. The U6 was used as the cytoplasmic control and MTMR1 as the nuclear control for RNA nucleus-cytoplasm split RT-qPCR. SP1 was used as the nuclear control and β-ACTIN as the cytoplasmic control for the nucleus-cytoplasm split western blot.

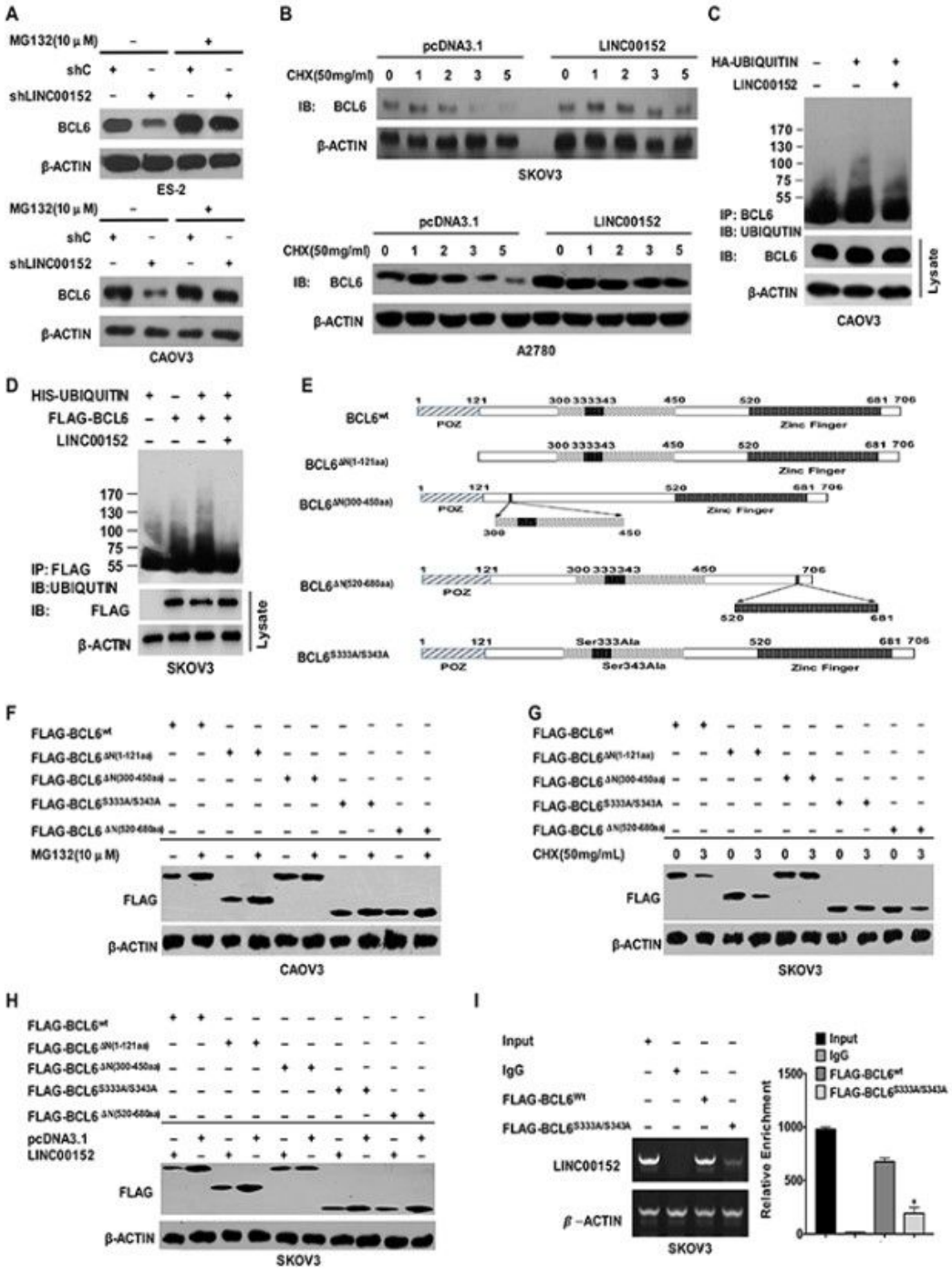

Figure 4

Figure 4

LINC00152 elevates the level of BCL6 protein by binding its specific sites and suppressing its ubiquitination A. The western blot results showed the rescued protein levels of BCL6 by MG132 (10 μM) in NC and LINC00152-knockdown ES-2 and CAOV3 cells. B. The western blot results showed the prolonged half-life of BCL6 protein in NC and LINC00152-overexpressing A2780 and SKOV3 cells under the influence of CHX (50 mg/mL) at indicated time points (Left). C. The in vivo ubiquitination assays

showed the endogenous polyubiquinated-BCL6 protein in NC and LINC00152-overexpressing CAOV3 cells. D. The in vivo ubiquitination assays showed the exogenous polyubiquinated-BCL6 protein in NC and LINC00152-overexpressing SKOV3 cells. E. The schematic diagram of full-length BCL6 protein and its mutants used in the study. The truncated domains and the mutated sites were shown. F. The western blot results showed the protein levels of wild-type BCL6 and its mutants under the influence of MG 132 (10 μM) in CAOV3 cells. G. The western blot results showed the protein levels of wild-type BCL6 and its mutants at the indicated time points under the influence of CHX (50mg/mL) in CAOV3 cells. H. The western blot results showed the protein levels of wild-type BCL6 and its mutants under the influence of LINC00152 overexpression in SKOV3 cells. I. The RNA immunoprecipitation assays showed the levels of LINC00152 precipitated by Flag-tagged wild-BCL6 and its mutant Flag-tagged BCL6S333A/S343A. The RT-qPCR products were turned to either electrophoresis or quantification by graph. *: $P<0.01$.

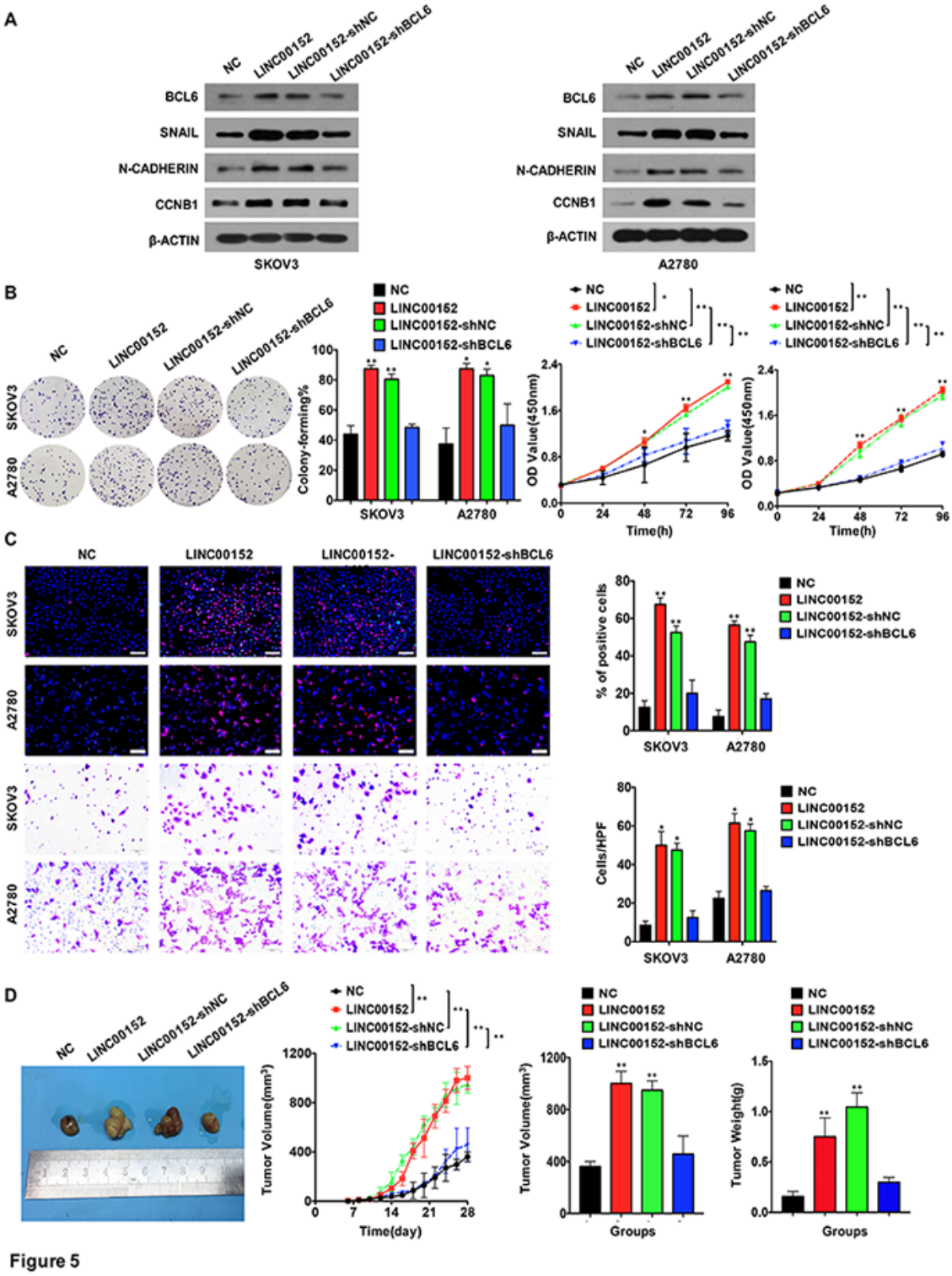

Figure 5

Figure 5

LINC00152 promotes ovarian cancer progression in a BCL6-mediated manner A. The western blot results of BCL6, SNAIL, N-CADHERIN and CCNB1 in the NC, LINC00152-overexpressing, LINC00152-shNC and LINC00152-shBCL6 SKOV3 and A2780 cells. B. Left: The representative images of colony-forming (Left) of NC, LINC00152-overexpressing, LINC00152-shNC and LINC00152-shBCL6 SKOV3 and A2780 cells for 14 days. *: P<0.05. **: P<0.01. Right: The CCK8 counting curves of NC, LINC00152-overexpressing,

LINC00152-shNC and LINC00152-shBCL6 SKOV3 and A2780 cells with the indicated time points. *: P<0.05. **: P<0.01. C. The representative images of EdU immunofluorescence (Top) and transwell assay (Bottom) in NC, LINC00152-overexpressing, LINC00152-shNC and LINC00152-shBCL6 infected SKOV3 and A2780 cells. The percentage of EdU positive cells were graphed under 100× and calculated under 200× magnification. The penetrated cells were graphed under 200× and counted under 400× magnification. *: P<0.05. **: P<0.01. D. The xenograft tumorigenesis results of NC, LINC00152-overexpressing, LINC00152-shNC and LINC00152-shBCL6 infected SKOV3 cells. Tumors were photographed and the speed of tumor growth was illustrated as curves, and the weights of tumors were calculated and analyzed. **: P<0.01.

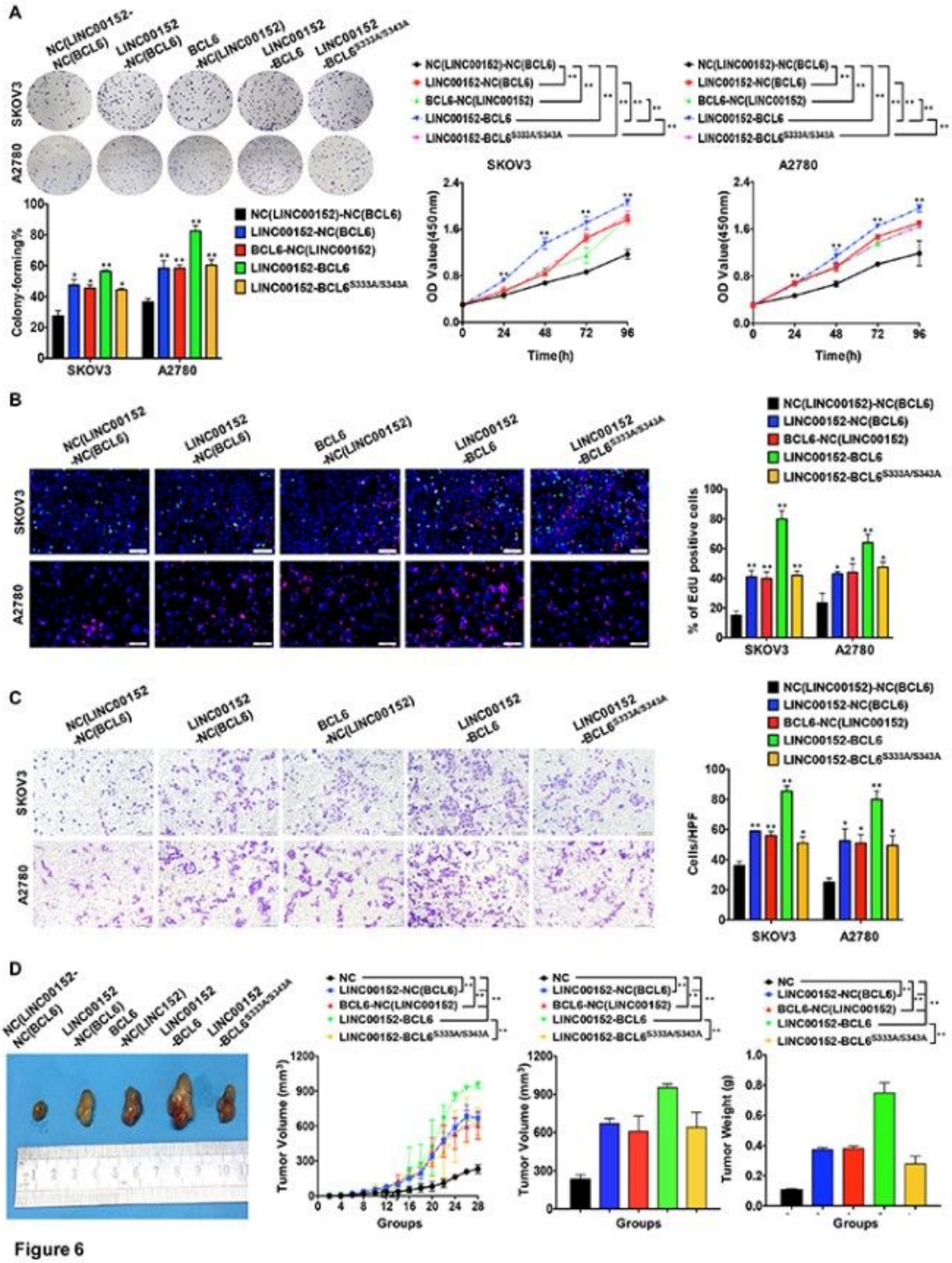

Figure 6

Figure 6

Ubiquitination-related sites are essential to LINC00152-BCL6 facilitated ovarian tumor progression A. Left: The representative images of colony-forming SKOV3 and A2780 cells infected with the lentivirus plasmids of NC, LINC00152-NC(BCL6), BCL6-NC(LINC00152), LINC00152-BCL6 and LINC00152-BCL6S333A/S343A for 14 days. *: P<0.05. **: P<0.01. Right: The CCK8 counting curves of SKOV3 and A2780 cells infected with the lentivirus plasmids of NC, LINC00152-NC(BCL6), BCL6-NC(LINC00152),

LINC00152-BCL6 and LINC00152-BCL6S333A/S343A with the indicated time points. **: P<0.01. B. The representative images of EdU immunofluorescence in NC, LINC00152-NC(BCL6), BCL6-NC(LINC00152), LINC00152-BCL6 and LINC00152-BCL6S333A/S343A SKOV3 and A2780 cells. The percentage of EdU positive cells were graphed under 100× and calculated under 200× magnification. *: P<0.05. **: P<0.01. C. The representative images of Transwell assay in NC, LINC00152-NC(BCL6), BCL6-NC(LINC00152), LINC00152-BCL6 and LINC00152-BCL6S333A/S343A SKOV3 and A2780 cells. The penetrated cells were graphed under 200× and counted under 400× magnification. *: P<0.05. **: P<0.01. The xenograft tumorigenesis results of NC, LINC00152-NC(BCL6), BCL6-NC(LINC00152), LINC00152-BCL6 and LINC00152-BCL6S333A/S343A infected SKOV3 cells. Tumors were photographed and the speed of tumor growth was illustrated as curves, and the weights of tumors were calculated and analyzed. **: P<0.01.

Supplementary Files

This is a list of supplementary files associated with this preprint. Click to download.

- Supplementary.docx